

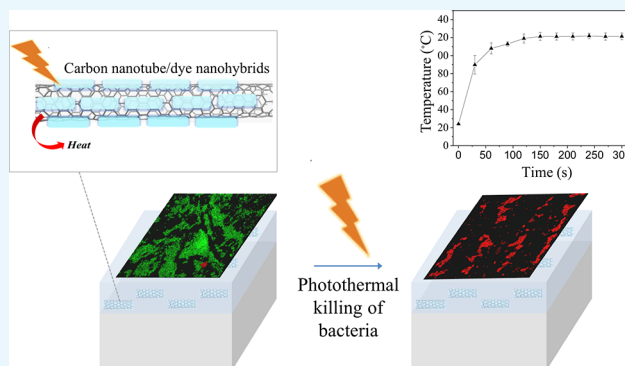
Fluorophore-Decorated Carbon Nanotubes with Enhanced Photothermal Activity as Antimicrobial Nanomaterials

Betul Oruc[†] and Hayriye Unal^{*,‡,Ⓜ}

[†]Faculty of Engineering and Natural Sciences and [‡]Sabanci University, SUNUM Nanotechnology Research Center, 34956 Istanbul, Turkey

Supporting Information

ABSTRACT: Alternative approaches to inactivate bacteria through physical damage provide an important solution to problems associated with colonization of material surfaces by antibiotic-resistant bacteria. Here, we present the utilization of carbon nanotubes functionalized with near-infrared (NIR)-absorbing fluorophores as effective photothermal agents that can kill bacteria through laser-activated heat generation. The array of 3,3'-diethylthiatricarbocyanine (DTTC) fluorophores self-assembled on the surface of multiwalled carbon nanotubes (MWNTs) acted as a light-harvesting antenna that increased the NIR light absorption and heat generation capacity of the MWNTs. The MWNT/DTTC nanohybrids generated elevated temperatures reaching 92 °C upon 15 min NIR laser irradiation, resulting in a 77% killing efficiency on *Pseudomonas aeruginosa* cells in dispersion. When the MWNT/DTTC nanohybrids were embedded into a waterborne polyurethane matrix, the resulting surface coatings presented temperatures reaching 120 °C in only 2 min of laser irradiation, where multiple laser irradiation cycles did not affect the generated temperature elevations. MWNT/DTTC–polyurethane nanocomposite coatings were also demonstrated to kill all *P. aeruginosa* cells attached to the surface, indicating their strong potential as light-activated antimicrobial and antibiofilm coatings.



INTRODUCTION

The contamination of materials and surfaces with pathogenic bacteria and biofilms constitutes an important challenge in various settings ranging from hospital environments to food processing facilities and necessitates an interdisciplinary research approach for creating solutions. The traditional approach of treating bacteria with biochemical tools such as antibiotics is not a viable option anymore as more bacterial strains have gained resistance to antibiotics.^{1,2} New approaches are needed that focus on the physical destruction of bacteria as alternatives to destruction of bacteria through biochemical pathways.

Photothermal therapy with the aid of functional nanomaterials that absorb light and release it in the form of heat through nonradiative relaxation provides a promising and effective alternative approach to kill bacteria. Light-induced heat generation around photothermal nanomaterials physically destroys bacteria through hyperthermia effects. Inorganic nanoparticles exhibiting localized surface plasmon resonance, such as various gold nanostructures, demonstrate strong photothermal properties and are widely utilized for killing bacteria.^{3–7} Similarly, some near-infrared (NIR) absorbing polymers and polyelectrolytes were also demonstrated as efficient photothermal agents.^{8–11} Another group of nanoparticles exhibiting photothermal properties due to their NIR

light absorption capacities are carbon-based nanoparticles such as carbon nanotubes^{12–15} and graphene.^{16–22} The inherent binding affinity of carbon nanotubes for bacteria¹² and their lower costs render them advantageous over gold nanoparticles as photothermal agents for killing bacteria. However, carbon nanotubes present significantly lower NIR light absorption capacity than gold nanostructures,²³ which make them inferior in terms of the NIR light-induced heat that they can generate. Thus, enhancing the NIR light absorption capacity of carbon nanotubes can result in new photothermal agents with higher NIR light absorption capacity and local heat generation, which can kill bacteria more effectively upon spontaneous interaction.

In this work, we focused on enhancing the NIR light absorption capacity of carbon nanotubes with fluorophores to obtain photothermal agents that generate heat and result in high temperature elevations while acting effectively against bacteria. How fluorophores interact with carbon nanotubes was attractive to researchers in various different aspects. Fluorophores were demonstrated to be useful as carbon nanotube dispersing agents,²⁴ electron donor–acceptor systems,^{25–27} quenchers in carbon nanotube-based fluorescent

Received: January 11, 2019

Accepted: March 6, 2019

Published: March 20, 2019

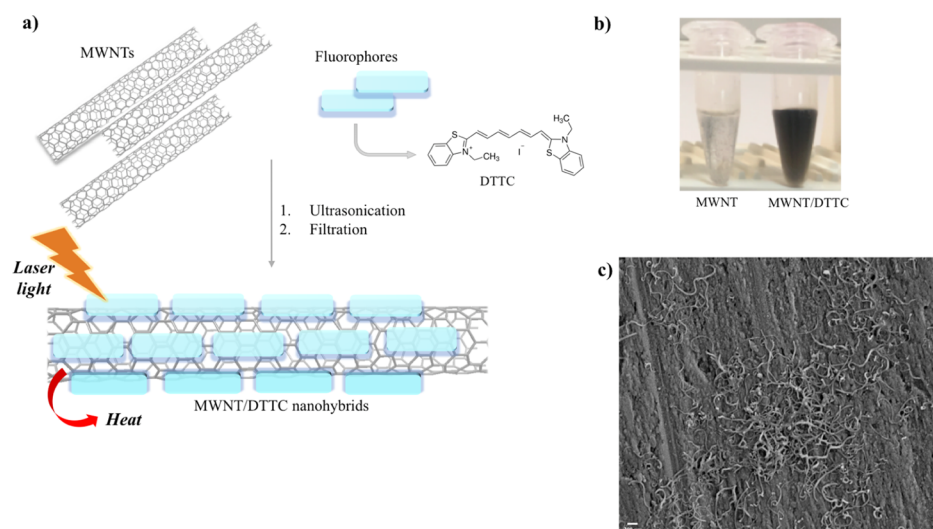


Figure 1. (a) Preparation of MWNT/DTTC nanohybrids. (b) Photographs of 0.02 mg/mL MWNTs sonicated in water (left) and in a 20 μ M aqueous solution of DTTC (right). (c) SEM micrograph of MWNT/DTTC nanohybrids.

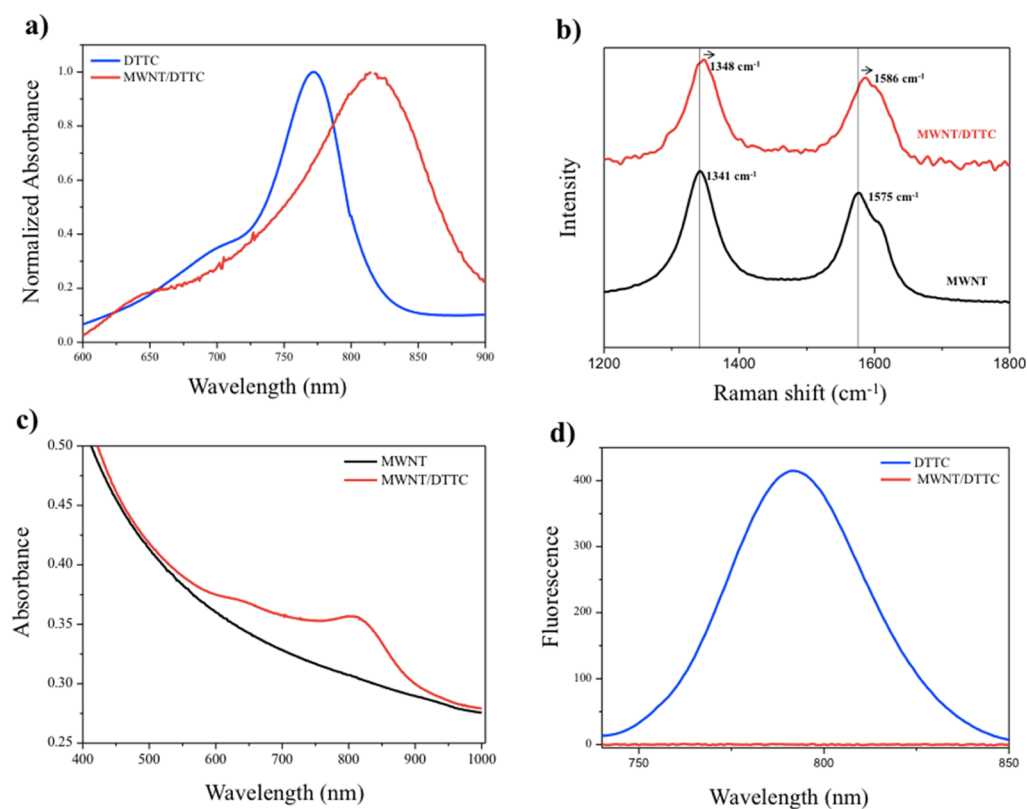


Figure 2. (a) Normalized absorbance spectra of DTTC and MWNT/DTTC containing equal concentrations of DTTC (20 μ M). (b) Raman spectra of MWNTs and MWNT/DTTC nanohybrids magnified in the G band region. (c) Absorbance spectra of MWNTs and MWNT/DTTC containing equal concentrations of MWNTs (0.01 mg/mL). (d) Fluorescence spectra of DTTC and MWNT/DTTC containing equal concentrations of DTTC (20 μ M).

sensors,^{28,29} or fluorescent labels for the visualization of carbon nanotubes.^{30–32} Fluorophores can interact with the sp^2 hybridized electronic system of carbon nanotubes through noncovalent interactions, such as π – π stacking or van der Waals or hydrophobic interactions, resulting in fluorophore/carbon nanotube hybrid structures with different functionalities that are easily tunable.

Here, we report the decoration of multiwalled carbon nanotubes (MWNTs) with fluorophores to enhance their NIR

light absorption capacity and photothermal effect, where fluorophores act as an antenna to increase the amount of light absorbed and the heat generated as a result of the photothermal conversion. The light-harvesting effect originating from fluorophores allows NIR irradiation-induced temperature elevations and bacteria killing rates that could not be reached by the irradiation of MWNTs only.

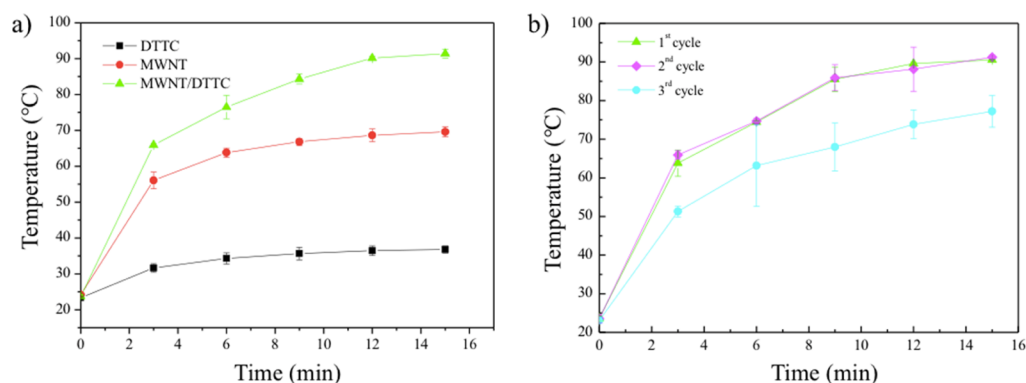


Figure 3. (a) Time–temperature curves of DTTC, MWNT, and MWNT/DTTC containing equal DTTC (20 μ M) and MWNT (0.01 mg/mL) concentrations generated by 808 nm NIR laser irradiation for 15 min at a laser power of 1 W/cm². (b) Time–temperature curves generated by 808 nm NIR laser irradiation of the same MWNT/DTTC nanohybrid sample for three consequent cycles.

RESULTS AND DISCUSSION

For the enhancement of their light absorption capacity in the NIR region, MWNTs were decorated with the NIR-absorbing carbocyanine dye, 3,3'-diethylthiatricarbocyanine (DTTC). As a symmetrical carbocyanine dye, exhibiting strong NIR light absorbing capacity and high resonance Raman cross section,³⁵ DTTC has been widely utilized as a fluorescent label in biomedical imaging^{36–38} and Raman label for surface-enhanced Raman spectroscopy.³⁹ On the basis of our previous studies that have demonstrated strong noncovalent interactions between UV–vis light absorbing carbocyanine dyes and MWNTs,³² we hypothesized that DTTC molecules, as NIR-absorbing carbocyanine dyes, will also strongly bind MWNTs. Here, DTTC molecules were utilized to build light-harvesting arrays on the surface of MWNTs to increase the amount of NIR light absorbed and converted to heat by MWNT/DTTC hybrids. MWNTs were dispersed in an aqueous solution of DTTC through ultrasonication followed by ultracentrifugation and filtration to remove aggregated forms of MWNTs that were not dispersed and unbound dye molecules (Figure 1a). Images of resulting MWNT/DTTC hybrids are demonstrated in Figure 1b. Although MWNTs alone were not dispersed in water under the same conditions, they were finely dispersed in an aqueous solution of DTTC molecules as can be seen by the darker color of the resulting stable mixtures. DTTC-assisted dispersion of MWNTs was visualized with scanning electron microscopy (SEM) (Figure 1c). MWNTs were individually dispersed presenting outer diameters in the range of 15–50 nm, larger than the diameters in the range of 13–18 nm, before functionalization with DTTC. DTTC molecules acted as strong dispersing agents that debundled the MWNTs, potentially because of strong noncovalent interactions, such as π – π stacking and van der Waals interactions, resulting in MWNTs decorated with dye molecules.

The MWNT/DTTC hybrids were demonstrated to be thermally stable up to approximately 65 °C by an isochronal temperature assay (Figure S1). Above this temperature, noncovalent bonds between MWNTs and DTTC molecules begin to break, resulting in aggregation of MWNTs. At 4 °C, the MWNT/DTTC hybrids remained stable for at least 4 months with less than 10% dissociation.

Noncovalent binding interactions between MWNTs and DTTC molecules were characterized by the absorption spectroscopy. The normalized absorption spectrum of free

DTTC molecules in aqueous solution was compared to the normalized absorption spectrum of MWNT/DTTC hybrids to comment on possible binding interactions (Figure 2a). The absorption spectrum of MWNT/DTTC hybrids demonstrated a bathochromic shift of 50 nm relative to free DTTC molecules, indicating a significant change in the electronic environment, which confirms noncovalent binding of DTTC molecules onto MWNTs. Previous studies on aggregates of dyes suggest that a bathochromic shift usually indicates a J-aggregate, where dye molecules form an edge-to-edge array on a template.⁴⁰ The fact that the absorption spectrum of DTTC molecules presented a similar shift implies that the DTTC molecules form an array on the MWNTs resulting in MWNTs decorated with fluorophores. Strong noncovalent interactions between MWNTs and DTTC molecules were further evidenced by changes in the electronic environment of MWNTs with Raman spectroscopy. Raman shift of the tangential stretch G band of the MWNT alone at 1575 cm⁻¹ exhibits an upshift to 1586 cm⁻¹ when DTTC molecules are bound to MWNTs (Figure 2b). This shift indicates a change in the electronic structure of sidewalls of the MWNTs through strong π – π interactions when the MWNT/DTTC nanohybrid structure is formed. Similar shifts in the G band upon noncovalent binding of molecules to MWNTs were reported previously.⁴¹ The effect of dye molecules on the absorption behavior of MWNTs was also investigated. Figure 2c demonstrates the absorption spectrum of the MWNT/DTTC hybrids in the NIR region in comparison to MWNTs dispersed in a surfactant solution. The MWNT/DTTC hybrids demonstrate an additional absorption peak that is not present in the absorbance spectrum of MWNTs, indicating that the presence of DTTC molecules have enhanced the absorption capacity of MWNTs in the NIR region. As more of the NIR light can be absorbed by MWNT/DTTC hybrids, they can potentially convert more of the light energy to heat energy resulting in higher temperature elevations when irradiated with a NIR laser.

NIR fluorescence spectra of the prepared hybrids were also analyzed in order to investigate conversion of the absorbed light energy into different forms of energy. Fluorescence emission of DTTC molecules that centered around 800 nm was completely quenched when they form hybrids with MWNTs; hybrids did not emit fluorescence light (Figure 2d). This result indicates that all light energy absorbed by

MWNT/DTTC hybrids was converted into heat energy, which makes them potential photothermal agents.

Photothermal properties of MWNT/DTTC hybrids were studied by measuring their NIR laser-activated temperature elevations as a result of heat generation. Aqueous dispersions of MWNTs and MWNT/DTTC hybrids were irradiated with 808 nm laser for 15 min while their temperatures were monitored. The dispersion of MWNTs reached only 69 °C from room temperature after 15 min of irradiation, whereas MWNT/DTTC hybrids reached 92 °C, demonstrating an additional 22 °C temperature elevation (Figure 3a). The array of DTTC molecules self-assembled on the surface of MWNTs enhanced the amount of NIR light absorbed and, thus, the amount of energy converted into heat, which caused significantly larger temperature elevations. Considering the fact that photothermal conversion efficiency is proportional to temperature rise at constant laser power,⁴² it can be stated that MWNT/DTTC nano hybrids presented a 61% improvement in photothermal conversion efficiency relative to MWNTs alone. It is also important to note that the temperature of a solution of free DTTC molecules did not present a significant temperature elevation upon irradiation with NIR laser light under the same conditions, confirming that large temperature elevations demonstrated by MWNT/DTTC hybrids are actually caused by the photothermal effect of hybrids and not by direct heating by the laser or the NIR absorption by DTTC molecules alone.

The multiple uses of MWNT/DTTC hybrids as photothermal agents were also important to study. Figure 3b presents heating curves obtained when the MWNT/DTTC hybrids that were already irradiated for 15 min with laser light and cooled down to room temperature were irradiated again for the second and third times. At the end of the second cycle of irradiation, the MWNT/DTTC hybrids were able to reach the same temperature that they reached in the first cycle, clearly demonstrating that the MWNT/DTTC hybrids remained stable at high temperatures; the array of DTTC molecules on the MWNTs did not dissociate. When the same hybrids were irradiated with laser light for the third time, the monitored temperature was only 70 °C, which is the same temperature monitored when MWNTs alone were irradiated for 15 min, indicating that DTTC molecules have started to dissociate from the MWNT template. Results obtained from this experiment show that MWNT/DTTC hybrids stay stable until they are exposed to laser light for a certain time; thus, they can be utilized in several rounds of shorter laser irradiation times to generate temperatures reaching above 90 °C. Once the MWNT/DTTC hybrids start to dissociate, they still cause temperature elevations but the generated heat is lower than the initial rounds.

The photothermal effect of MWNT/DTTC hybrids was demonstrated with their ability to kill bacteria. The laser-activated antimicrobial properties of MWNT/DTTC hybrids were tested on *Pseudomonas aeruginosa*, as a Gram-negative model microorganism. *P. aeruginosa* treated with MWNT and MWNT/DTTC dispersions of equal concentrations along with *P. aeruginosa* that are not treated were irradiated with NIR laser for 15 min. Viabilities of cells before and after laser irradiation were determined by LIVE/DEAD staining, where *P. aeruginosa* cell sample before laser treatment was designated as the reference for 100% viability (Figure 4). The MWNTs presented antimicrobial activity on *P. aeruginosa* even before the laser treatment as can be seen by the lower viability value

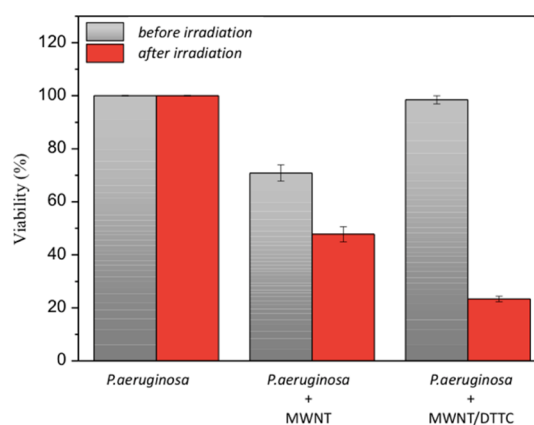


Figure 4. Viability of *P. aeruginosa* cells (2×10^8 cfu/mL) in the presence and absence of 0.01 mg/mL MWNTs and MWNT/DTTC nano hybrids before and after 808 nm laser irradiation for 15 min.

compared to cells that are not treated with the MWNTs. Such antimicrobial effect of MWNTs because of their noncovalent interactions with bacterial cell walls was reported earlier.⁴³ The MWNT/DTTC hybrids, on the other hand, did not present any antimicrobial activity on *P. aeruginosa* cells before the laser treatment. The array of DTTC molecules formed on the surface of MWNTs possibly prevents interactions of MWNTs with cells and shields the toxic effect. The viability of bacteria treated with MWNTs and MWNT/DTTC hybrids after NIR laser treatment demonstrated the photothermal effect of these nanostructures. In the absence of MWNTs or MWNT/DTTC hybrids, *P. aeruginosa* were not killed under the same conditions, confirming that the NIR laser irradiation itself does not present any toxic effect on bacteria. When MWNTs in the bacterial suspension were irradiated with NIR laser light for 15 min, 52% of *P. aeruginosa* cells were killed in the suspension because of their inherent photothermal effect. On the other hand, when *P. aeruginosa* treated with MWNT/DTTC hybrids were irradiated with NIR laser light, the killing efficiency was 77%, indicating that the MWNTs decorated with DTTC molecules presented enhanced photothermal effect resulting in significantly stronger laser-activated antimicrobial activity than MWNTs only. The enhanced absorption capacity of the MWNT/DTTC hybrids enabled by the array of DTTC molecules formed on MWNTs resulted in larger laser light-activated temperature elevations and higher antimicrobial activity.

Applied NIR laser light energy was absorbed and converted to heat by MWNTs and MWNT/DTTC nano hybrids, resulting in elevated local temperatures. Most of the bacterial cells that were in contact with MWNTs and MWNT/DTTC nano hybrids died through hyperthermia as their cell walls were physically damaged at increasing temperatures. A similar laser-activated antimicrobial activity was observed when the prepared nano hybrids were tested against *Staphylococcus aureus*, a Gram-positive species, demonstrating that both Gram negative and Gram-positive bacteria can be deactivated through the physical damage caused by these nano hybrids (Figure S2). Killing efficiency of the nano hybrids was demonstrated to decrease when their concentration was lowered, proving that bacterial killing was indeed caused by the NIR laser-activated photothermal effect and not by the NIR laser itself, as shown in Figure S3. The duration of NIR laser irradiation also affected the viability of nano hybrid-

treated bacteria, where shorter laser irradiation times resulted in less killing efficiency (Figure S4). We believe that the killing efficiency can be improved further by experimental conditions such as shaking or manipulation of the container volume to obtain a more homogeneous distribution of the laser light and better heat transfer.

The physical destruction of bacteria through the heat generated by the MWNT/DTTC hybrids after the laser treatment is also demonstrated by SEM. Figure 5 presents *P.*

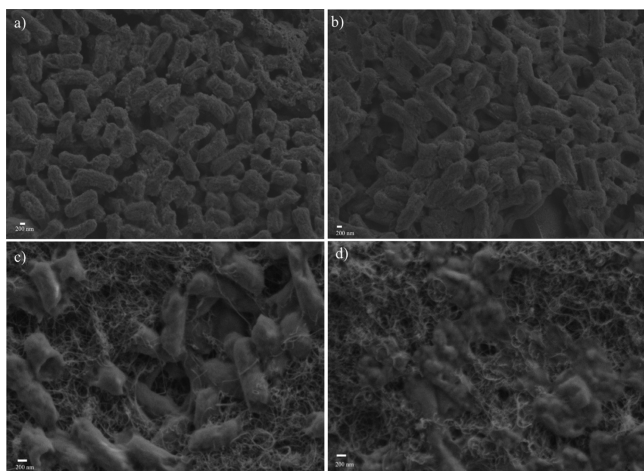


Figure 5. Representative SEM images of *P. aeruginosa* cells alone (a,b) and *P. aeruginosa* cells treated with 0.01 mg/mL MWNT/DTTC nanohybrids (c,d). Images (a,c) were obtained before 808 nm laser irradiation; images (b,d) were obtained after 808 nm laser irradiation.

aeruginosa cells alone and *P. aeruginosa* cells treated with MWNT/DTTC hybrids before and after the NIR laser treatment. The control sample including only cells did not exhibit any structural deformation after the laser treatment, confirming that the direct absorption of NIR laser light does not present any toxicity on cells. When the cells are treated with MWNT/DTTC hybrids followed by laser irradiation for 15 min, their structures were deformed, where outlines of cells mostly disappeared. Extensive temperature elevations caused

by the MWNT/DTTC hybrids lead to lysis of cell walls potentially because of heat activated protein denaturation.

MWNT/DTTC hybrids exhibiting strong light-activated antimicrobial activity were incorporated into water-based polyurethane (PU) coating materials in order to evaluate their activity on surfaces as antimicrobial and antibiofilm coatings that can kill attached bacteria upon NIR laser irradiation (Figure 6). As attractive environmentally friendly polymeric materials that can be designed to be biocompatible, waterborne PUs have been demonstrated to have excellent thermal and mechanical properties and are widely utilized as stable coatings for biomedical applications.⁴⁴ Nanocomposites of MWNT/DTTC hybrids and waterborne PU can potentially be applied as light-activated coatings for material surfaces that are prone to colonization by bacteria. Aqueous PU dispersions composed of polyester-based PU were blended with MWNTs and MWNT/DTTC nanohybrids resulting in nanocomposites containing 0.001 wt % MWNTs homogeneously distributed within the PU matrix. Photothermal activity of MWNT/DTTC-PU nanocomposites were demonstrated on self-standing cast films demonstrated in Figure 6 (inset).

The photothermal activity of MWNT-PU and MWNT/DTTC-PU nanocomposite films were determined by measuring the temperature elevation upon NIR laser irradiation. Figure 7a demonstrates that the temperature of MWNT/DTTC-PU film quickly raised up to 120 °C within 2 min of laser irradiation. On the other hand, the MWNT-PU film was also heated up within the same period of laser irradiation; however, it presented a 30 °C lower temperature, indicating that the presence of DTTC dye array around the MWNTs significantly increases their photothermal effect even when embedded within a polymer matrix. The PU film without MWNTs did not present an increase in temperature, confirming that elevated temperatures were caused by the photothermal activity of MWNTs or MWNT/DTTC hybrids. MWNT/DTTC nanohybrids embedded within the PU matrix resulted in much higher temperature increase than the same amount of MWNT/DTTC nanohybrids in aqueous dispersion, potentially because of the lower heat conductivity of the polymeric material compared to the aqueous environment. The heat released from the MWNT/DTTC nanohybrids is

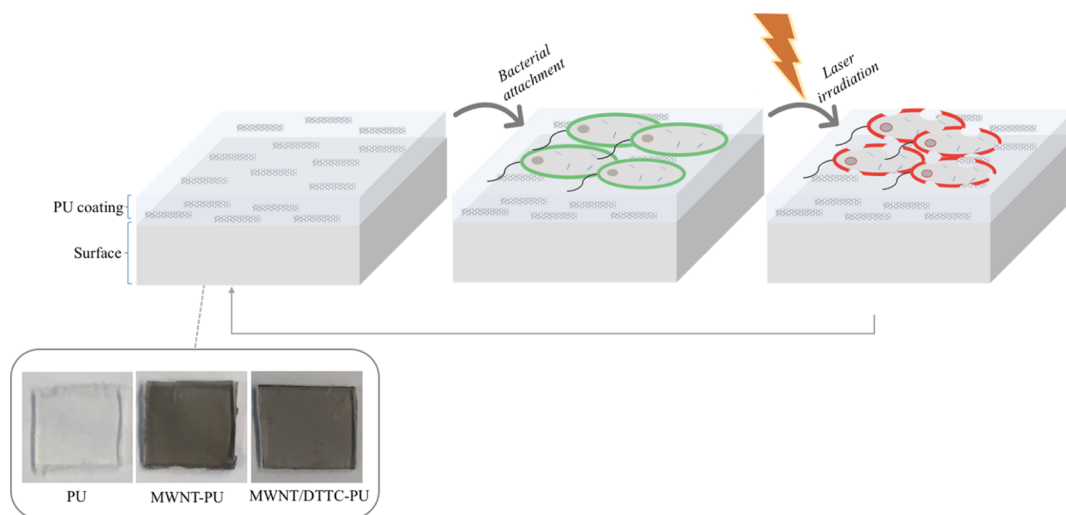


Figure 6. Schematic demonstration of the application of MWNT/DTTC-PU nanocomposites as antimicrobial surface coatings. Inset: Photographs of PU, MWNT-PU, and MWNT/DTTC-PU nanocomposites as self-standing films.

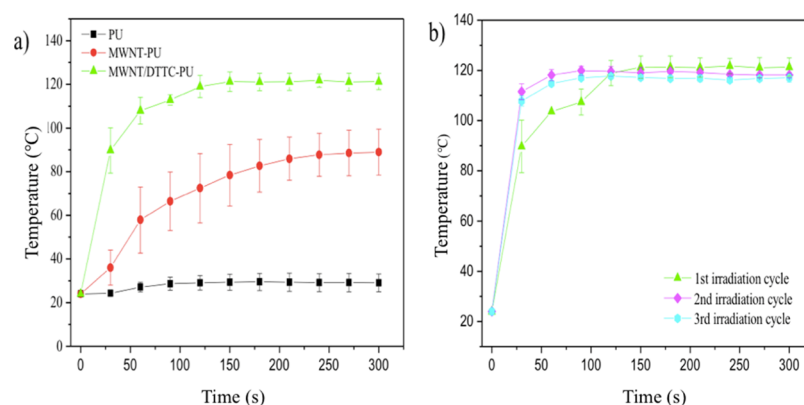


Figure 7. (a) Time–temperature curves of PU, MWNT–PU, and MWNT/DTTC–PU films containing 0.001 wt % MWNTs and MWNT/DTTC nanohybrids generated by 808 nm NIR laser irradiation for 5 min. (b) Time–temperature curves generated by 808 nm NIR laser irradiation of the same MWNT/DTTC–PU film for three consecutive cycles.

trapped in the PU matrix resulting in higher measured temperatures. High temperatures generated by these coating materials make them excellent candidates for antimicrobial surfaces as these temperatures would present a toxic effect to most of bacterial species. The potential of MWNT/DTTC–PU nanocomposites as reusable surface coatings retaining photothermal activity upon multiple laser treatments was also investigated (Figure 7b). When MWNT/DTTC–PU films that were already irradiated with laser for 5 min were irradiated again for the second and third time, they reached the same elevated temperature of 120 °C as in the first cycle. MWNT/DTTC nanohybrids that started dissociating after a certain duration of laser exposure in aqueous dispersions remained stable when embedded in the polymer matrix. These results indicate that these materials can be applied onto surfaces where bacterial attachment reoccur and bacterial inactivation is needed multiple times.

The ability of the laser-activated antimicrobial activity of MWNT/DTTC–PU coating materials to kill the surface-attached bacteria upon NIR laser irradiation was also investigated. MWNT/DTTC–PU films were incubated with *P. aeruginosa* overnight in static growth conditions for 24 h to allow adhesion of bacteria onto film surfaces followed by staining with live/dead cell indicator dyes. The stained surfaces were imaged with laser scanning confocal microscopy before and after NIR laser irradiation for 15 min. Representative images are shown in Figure 8. Although bacteria attached to the PU surface remained alive following the NIR laser irradiation for 15 min, all bacteria attached to the MWNT/DTTC–PU surface were killed upon the laser treatment. The temperature increase on the MWNT/DTTC–PU surface during the laser irradiation physically damaged and killed the attached bacteria, demonstrating the potential of these surfaces as antibiofilm surfaces that can eradicate established biofilms.

CONCLUSIONS

We presented the decoration of MWNTs with NIR light absorbing fluorophores to enhance their light absorbing capacity with the aim of improving their photothermal properties. DTTC fluorophores formed strong noncovalent interactions with MWNTs and formed a self-assembled array, which acted as light-harvesting antennas increasing the amount of laser light absorbed by the resulting MWNT/DTTC nanohybrids. The enhanced light absorption by the MWNT/DTTC nanohybrids was reflected as enhanced heat generation

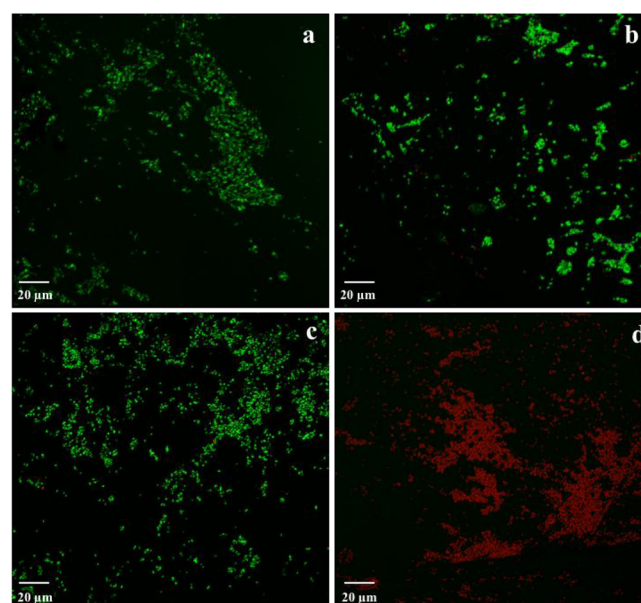


Figure 8. Representative laser scanning confocal microscopy images of PU (a,b) and MWNT/DTTC–PU surfaces containing 0.001 wt % MWNT/DTTC nanohybrids (c,d) incubated with 2×10^8 cfu/mL *P. aeruginosa*. Images (a,c) were obtained before 808 nm laser irradiation; images (b,d) were obtained after 808 nm laser irradiation.

resulting in elevated temperatures that cannot be reached by MWNTs alone under the same laser irradiation conditions. The irradiation of *P. aeruginosa* suspensions in the presence of MWNT/DTTC nanohybrids resulted in 77% killing of bacteria through the hyperthermal physical damage as demonstrated by SEM. Nanocomposites of waterborne PU and MWNT/DTTC were shown as potential antimicrobial and antibiofilm coating materials, which can generate temperatures reaching 120 °C and kill surface attached bacteria upon laser irradiation repeatedly. Photothermal agents based on fluorophore-enhanced carbon nanotubes and their surface coatings presented here have strong potential as antimicrobial and antibiofilm nanomaterials effective on antibiotic-resistant bacteria.

EXPERIMENTAL SECTION

Materials. MWNTs with 13–18 nm outer diameter, 3–30 μm length, and 99 wt % purity were provided by Cheap Tubes

Inc. (Cambridgeport, VT, USA). 3,3'-Diethylthiatricarbocyanine iodide (DTTC, 99%) was purchased from Sigma-Aldrich (Germany). Triton X-100 was purchased from Merck Millipore (Darmstadt, Germany). *P. aeruginosa* (ATCC 27853) and *S. aureus* (ATCC 29213) were purchased from Medimark (France). Nutrient broth (NB) was purchased from Biolife (Milano, Italia). The LIVE/DEAD BacLight bacterial viability kit (L7012) was purchased from Life Technologies (Carlsbad, CA, USA). Centrifugal filter devices (30 kDa cutoff, Microcon) were purchased from Millipore (MA, USA). Anionic, aqueous PU dispersion based on a polyester-polyol was kindly supplied by Punova R&D and Chemicals Inc. (Turkey) with a 35 wt % solid content.

Preparation of MWNT and MWNT/DTTC Nanohybrids. A dispersal solution (10 mL) containing 0.2 mg/mL MWNTs and 20 μM DTTC was sonicated in an ice-bath with a microprobe (QSonica, Q700) for 20 min with 4 s pulse on and 5 s pulse off time at a power of 4–5 W. For the preparation of MWNT sample, the same amount of MWNT was dispersed in water containing 5 wt % Triton X-100 under the same conditions. Aqueous dispersions were centrifuged at 5000 rpm for 5 min to remove MWNTs that were not dispersed. The black-colored supernatant was pipetted into a clean falcon tube. Removal of unbound dye molecules was performed using Microcon centrifugal filters according to manufacturer's instructions. Concentration of MWNT and MWNT/DTTC dispersions were determined by absorbance spectroscopy (Cary 5000 spectrophotometer) using the specific extinction coefficient for MWNTs at 500 nm ($\epsilon_{500} = 46 \text{ mL}\cdot\text{mg}^{-1}\cdot\text{cm}^{-1}$).³³

Characterization of MWNT/DTTC Nanohybrids. Absorbance spectroscopy was performed to confirm the increase in absorbance capacity after nanohybrid formation. Samples were scanned in a quartz cuvette in the wavelength range of 200–1000 nm.

For Raman spectroscopy, dispersion samples were air-dried on silicon wafers and measurements were made on a Renishaw inVia Reflex Raman spectrometer equipped with a 532 nm laser.

Fluorescence spectra of the nanohybrids were obtained with a Cary Eclipse fluorescence spectrophotometer. DTTC and MWNT/DTTC were scanned in a quartz cuvette at 720 nm excitation.

Thermal stability of the MWNT/DTTC nanohybrids was determined by an isochronal temperature assay,³⁴ where the MWNT/DTTC samples were incubated at varied temperatures and MWNT aggregation after a fixed length of time was determined. MWNT/DTTC dispersions were aliquoted in 40 μL volume in Eppendorf tubes and incubated for 10 min at designated temperatures (23–95 $^{\circ}\text{C}$) to remove MWNT bundles. Supernatants were carefully collected and absorption at 500 nm was determined. The fraction of MWNT/DTTC was calculated by dividing the absorbance of MWNT/DTTC nanohybrids that remained dispersed after centrifugation by that of the initial hybrid dispersion at 4 $^{\circ}\text{C}$.

Laser-Activated Heat Generation in MWNT/DTTC Nanohybrids. For an accurate comparison of laser-activated heat generation by MWNT versus MWNT/DTTC, corresponding dispersions with equal MWNT concentrations (0.01 mg/mL) were prepared. A DTTC solution (1.2 mL, 20 μM) only, MWNT dispersion only and MWNT/DTTC dispersion were exposed to continuous laser irradiation with a laser power of 1 W/cm^2 at 808 nm for 15 min (STEMINC,

SMM22808E1200) (Doral, FL USA). Temperature was recorded every 3 min with a thermocouple (Hanna HI 935005 K-thermocouple thermometer). The thermocouple was immersed in the dispersion without blocking the path of the laser beam to avoid direct heating of the thermocouple by irradiation of the laser light.

Laser-Activated Antimicrobial Activity of MWNT/DTTC Hybrids. Overnight cultures (3 mL) of *P. aeruginosa* were grown in NB medium at 37 $^{\circ}\text{C}$ in a shaker incubator. The cells were washed twice by centrifugation at 5000 rpm for 5 min and resuspended in sterile phosphate-buffered saline (PBS). Bacterial suspensions (2×10^8 cfu/mL) were mixed with dispersions of MWNTs and MWNT/DTTC nanohybrids containing 0.01 mg/mL MWNTs immediately before laser irradiation. A control sample containing the same number of bacteria in 1.2 mL of water was also prepared and labeled as “cells only”. Two sets of “cells only”, “*P. aeruginosa*-MWNT”, and “*P. aeruginosa*-MWNT/DTTC” mixtures were prepared to investigate the photothermal destruction of bacteria during laser treatment. While the first set was irradiated with 808 nm NIR laser light for 15 min, the second set was kept in ice. The viability of *P. aeruginosa* in prepared samples before and after laser irradiation was determined by using the LIVE/DEAD viability assay. Each sample (0.1 mL) was transferred into a 96-well plate and stained with LIVE/DEAD BacLight kit for 20 min in the dark at room temperature. The ratio of fluorescence intensity of live cells (SYTO 9, ex/em \approx 480/500 nm) to the fluorescence intensity of dead cells (propidium iodide, ex/em \approx 490/635 nm) was calculated for each sample. Fluorescence intensities at 538 and 612 nm were measured with a Fluoroskan Ascent FL microplate reader (Thermo Labsystems). Live/dead cell ratio of the “cells only” sample that was not irradiated with the laser was specified as 100% cell viability. The viability of each sample was determined in comparison to this reference sample. Experiments were conducted in triplicates. Postlaser viability was calculated as the ratio of viability after laser irradiation to viability before laser irradiation.

Scanning Electron Microscopy. MWNT/DTTC nanohybrids (20 μL , 0.01 mg/mL) were transferred onto an aluminum stub and air dried. Secondary electron images of gold-palladium-coated samples were obtained with a Zeiss Leo SUPRA 35 scanning electron microscope.

Following the viability assay, samples composed of *P. aeruginosa* and *P. aeruginosa*-MWNT/DTTC were centrifuged at 14 000 rpm for 5 min, and the supernatant was removed. The pellet containing the cells and MWNT/DTTC were fixed in 2.5% glutaraldehyde in sterile PBS for 2 h at room temperature. The cells were rinsed twice with sterile PBS followed by dehydration through a series of increasing ethanol concentrations. Pellets were transferred onto aluminum SEM stubs and air dried. Secondary electron images of samples were obtained with a Zeiss Leo SUPRA 35 scanning electron microscope.

Preparation of MWNT/DTTC-PU Coatings. MWNT/DTTC-PU nanocomposite coatings were prepared to investigate the photothermal activity of nanohybrids in surface coatings. Aqueous PU dispersion (3 g) with a solid content of 35% was thoroughly mixed with 2 mL of MWNT and MWNT/DTTC dispersions containing 0.006 mg/mL MWNTs under overhead agitation and allowed to mix for 1 h, resulting in 0.001 wt % MWNTs in solid PU. MWNT-PU and MWNT/DTTC-PU dispersions were cast onto Petri

dishes and dried overnight in an oven at 50 °C to evaporate the water content and produce self-standing nanocomposite films. A PU film prepared by the same procedure without adding the MWNT dispersion was used as a control. Each film was cut into 1 × 1 cm pieces for further experiments.

Laser-Activated Heat Generation in MWNT/DTTC–PU Coatings. K type cable thermocouple was fixed in place between a Teflon plate and a piece of film (1 × 1 cm) for each sample. PU, MWNT–PU, and MWNT/DTTC–PU films were exposed to continuous laser irradiation with a laser power of 1 W/cm² at 808 nm for 3 min. The temperature was recorded every 30 s. During the laser irradiation, the thermocouple heated up due to direct absorption of laser light. To correct for this direct heating effect, the maximum temperature reached by the thermocouple itself in the exact same experimental setup was determined and subtracted from each data point when generating the time–temperature curves.

Laser-Activated Antibiofilm Properties of MWNT/DTTC–PU Coatings. After wiping PU film surfaces with ethanol, they were incubated with 2 mL of *P. aeruginosa* suspension containing 2 × 10⁸ cfu/mL in a 12-well plate overnight at 37 °C without shaking. The culture medium with nonadherent bacteria was removed, and the films were gently washed twice with sterile PBS. The films were stained using LIVE/DEAD BacLight kit and incubated for 10 min in the dark at room temperature. The excess staining solution was rinsed with PBS. The films were mounted onto coverslips and examined with a Carl Zeiss LSM 710 laser scanning confocal microscope equipped with a Plan-Apochromat 63×/1.40 oil objective before and after exposure to NIR laser light for 15 min. Reported images are 3-D renderings of Z-stacks created by using the Zen 2010 software.

■ ASSOCIATED CONTENT

Supporting Information

The Supporting Information is available free of charge on the ACS Publications website at DOI: 10.1021/acsomega.9b00099.

Thermal stability of MWNT/DTTC nanohybrids, viability of *S. aureus* treated with MWNTs and MWNT/DTTC nanohybrids, and postlaser viability of MWNTs and MWNT/DTTC hybrids at different MWNT concentrations and different laser irradiation times (PDF)

■ AUTHOR INFORMATION

Corresponding Author

*E-mail: hunal@sabanciuniv.edu.

ORCID

Hayriye Unal: 0000-0002-9090-2440

Notes

The authors declare no competing financial interest.

■ ACKNOWLEDGMENTS

This work was supported by the Scientific and Technological Research Council of Turkey (TUBITAK) under the project number 315M235.

■ REFERENCES

(1) Norrby, S. R.; Nord, C. E.; Finch, R. Lack of Development of New Antimicrobial Drugs: A Potential Serious Threat to Public Health. *Lancet Infect. Dis.* **2005**, *5*, 115–119.

(2) Leeb, M. Antibiotics: A Shot in the Arm. *Nature* **2004**, *431*, 892–893.

(3) Kim, C.-B.; Yi, D. K.; Kim, P. S. S.; Lee, W.; Kim, M. J. Rapid Photothermal Lysis of the Pathogenic Bacteria, *Escherichia coli* Using Synthesis of Gold Nanorods. *J. Nanosci. Nanotechnol.* **2009**, *9*, 2841–2845.

(4) Khantamat, O.; Li, C.-H.; Yu, F.; Jamison, A. C.; Shih, W.-C.; Cai, C.; Lee, T. R. Gold Nanoshell-Decorated Silicene Surfaces for the Near-Infrared (NIR) Photothermal Destruction of the Pathogenic Bacterium *E. Faecalis*. *ACS Appl. Mater. Interfaces* **2015**, *7*, 3981–3993.

(5) Meeker, D. G.; Jenkins, S. V.; Miller, E. K.; Beenken, K. E.; Loughran, A. J.; Powless, A.; Muldoon, T. J.; Galanzha, E. I.; Zharov, V. P.; Smeltzer, M. S.; et al. Synergistic Photothermal and Antibiotic Killing of Biofilm-Associated *Staphylococcus aureus* Using Targeted Antibiotic-Loaded Gold Nanoconstructs. *ACS Infect. Dis.* **2016**, *2*, 241–250.

(6) Huang, W.-C.; Tsai, P.-J.; Chen, Y.-C. Functional Gold Nanoparticles as Photothermal Agents for Selective-Killing of Pathogenic Bacteria. *Nanomedicine* **2007**, *2*, 777–787.

(7) Sean Norman, R.; Stone, J. W.; Gole, A.; Murphy, C. J.; Sabo-Attwood, T. L. Targeted Photothermal Lysis of the Pathogenic Bacteria, *Pseudomonas Aeruginosa*, with Gold Nanorods. *Nano Lett.* **2008**, *8*, 302–306.

(8) Kim, S. H.; Kang, E. B.; Jeong, C. J.; Sharker, S. M.; In, I.; Park, S. Y. Light Controllable Surface Coating for Effective Photothermal Killing of Bacteria. *ACS Appl. Mater. Interfaces* **2015**, *7*, 15600–15606.

(9) Hsiao, C.-W.; Chen, H.-L.; Liao, Z.-X.; Sureshbabu, R.; Hsiao, H.-C.; Lin, S.-J.; Chang, Y.; Sung, H.-W. Effective Photothermal Killing of Pathogenic Bacteria by Using Spatially Tunable Colloidal Gels with Nano-Localized Heating Sources. *Adv. Funct. Mater.* **2015**, *25*, 721–728.

(10) Ju, E.; Li, Z.; Li, M.; Dong, K.; Ren, J.; Qu, X. Functional Polypyrrole–Silica Composites as Photothermal Agents for Targeted Killing of Bacteria. *Chem. Commun.* **2013**, *49*, 9048.

(11) Feng, G.; Mai, C.-K.; Zhan, R.; Bazan, G. C.; Liu, B. Narrow Band Gap Conjugated Polyelectrolytes for Photothermal Killing of Bacteria. *J. Mater. Chem. B* **2015**, *3*, 7340–7346.

(12) Kim, J.-W.; Shashkov, E. V.; Galanzha, E. I.; Kotagiri, N.; Zharov, V. P. Photothermal Antimicrobial Nanotherapy and Nano-diagnostics with Self-Assembling Carbon Nanotube Clusters. *Lasers Surg. Med.* **2007**, *39*, 622–634.

(13) Akasaka, T.; Matsuoka, M.; Hashimoto, T.; Abe, S.; Uo, M.; Watari, F. The Bactericidal Effect of Carbon Nanotube/Agar Composites Irradiated with near-Infrared Light on Streptococcus Mutans. *Mater. Sci. Eng., B* **2010**, *173*, 187–190.

(14) Levi-Polyachenko, N.; Young, C.; MacNeill, C.; Braden, A.; Argenta, L.; Reid, S. Eradicating Group A Streptococcus Bacteria and Biofilms Using Functionalised Multi-Wall Carbon Nanotubes. *Int. J. Hyperthermia* **2014**, *30*, 490–501.

(15) Ondera, T. J.; Hamme, A. T., II A Gold Nanopopcorn Attached Single-Walled Carbon Nanotube Hybrid for Rapid Detection and Killing of Bacteria. *J. Mater. Chem. B* **2014**, *2*, 7534–7543.

(16) Akhavan, O.; Ghaderi, E.; Efsandiari, A. Wrapping Bacteria by Graphene Nanosheets for Isolation from Environment, Reactivation by Sonication, and Inactivation by Near-Infrared Irradiation. *J. Phys. Chem. B* **2011**, *115*, 6279–6288.

(17) Jia, X.; Ahmad, I.; Yang, R.; Wang, C. Versatile Graphene-Based Photothermal Nanocomposites for Effectively Capturing and Killing Bacteria, and for Destroying Bacterial Biofilms. *J. Mater. Chem. B* **2017**, *5*, 2459–2467.

(18) Lin, D.; Qin, T.; Wang, Y.; Sun, X.; Chen, L. Graphene Oxide Wrapped SERS Tags: Multifunctional Platforms toward Optical Labeling, Photothermal Ablation of Bacteria, and the Monitoring of Killing Effect. *ACS Appl. Mater. Interfaces* **2014**, *6*, 1320–1329.

(19) Turcheniuk, K.; Hage, C.-H.; Spadavecchia, J.; Serrano, A. Y.; Larroulet, I.; Pesquera, A.; Zurutuza, A.; Pisfil, M. G.; Hélot, L.; Boukaert, J.; et al. Plasmonic Photothermal Destruction of Uropathogenic *E. Coli* with Reduced Graphene Oxide and Core/

Shell Nanocomposites of Gold Nanorods/Reduced Graphene Oxide. *J. Mater. Chem. B* **2015**, *3*, 375–386.

(20) Kurapati, R.; Vaidyanathan, M.; Raichur, A. M. Synergistic Photothermal Antimicrobial Therapy Using Graphene Oxide/Polymer Composite Layer-by-Layer Thin Films. *RSC Adv.* **2016**, *6*, 39852–39860.

(21) Wu, M.-C.; Deokar, A. R.; Liao, J.-H.; Shih, P.-Y.; Ling, Y.-C. Graphene-Based Photothermal Agent for Rapid and Effective Killing of Bacteria. *ACS Nano* **2013**, *7*, 1281–1290.

(22) Hui, L.; Auletta, J. T.; Huang, Z.; Chen, X.; Xia, F.; Yang, S.; Liu, H.; Yang, L. Surface Disinfection Enabled by a Layer-by-Layer Thin Film of Polyelectrolyte-Stabilized Reduced Graphene Oxide upon Solar Near-Infrared Irradiation. *ACS Appl. Mater. Interfaces* **2015**, *7*, 10511–10517.

(23) Kim, J.-W.; Galanzha, E. I.; Shashkov, E. V.; Moon, H.-M.; Zharov, V. P. Golden Carbon Nanotubes as Multimodal Photoacoustic and Photothermal High-Contrast Molecular Agents. *Nat. Nanotechnol.* **2009**, *4*, 688–694.

(24) Koh, B.; Kim, G.; Yoon, H. K.; Park, J. B.; Kopelman, R.; Cheng, W. Fluorophore and Dye-Assisted Dispersion of Carbon Nanotubes in Aqueous Solution. *Langmuir* **2012**, *28*, 11676–11686.

(25) Guldi, D. M.; Rahman, G. M. A.; Zerbetto, F.; Prato, M. Carbon Nanotubes in Electron Donor–Acceptor Nanocomposites. *Acc. Chem. Res.* **2005**, *38*, 871–878.

(26) Ballesteros, B.; de la Torre, G.; Ehli, C.; Aminur Rahman, G. M.; Agulló-Rueda, F.; Guldi, D. M.; Torres, T. Single-Wall Carbon Nanotubes Bearing Covalently Linked Phthalocyanines – Photoinduced Electron Transfer. *J. Am. Chem. Soc.* **2007**, *129*, 5061–5068.

(27) Casey, J. P.; Bachilo, S. M.; Weisman, R. B. Efficient photosensitized energy transfer and near-IR fluorescence from porphyrin-SWNT complexes. *J. Mater. Chem.* **2008**, *18*, 1510.

(28) Satishkumar, B. C.; Brown, L. O.; Gao, Y.; Wang, C.-C.; Wang, H.-L.; Doorn, S. K. Reversible Fluorescence Quenching in Carbon Nanotubes for Biomolecular Sensing. *Nat. Nanotechnol.* **2007**, *2*, 560–564.

(29) Yang, R.; Jin, J.; Chen, Y.; Shao, N.; Kang, H.; Xiao, Z.; Tang, Z.; Wu, Y.; Zhu, Z.; Tan, W. Carbon Nanotube-Quenched Fluorescent Oligonucleotides: Probes That Fluoresce upon Hybridization. *J. Am. Chem. Soc.* **2008**, *130*, 8351–8358.

(30) Yoshimura, S. H.; Khan, S.; Maruyama, H.; Nakayama, Y.; Takeyasu, K. Fluorescence Labeling of Carbon Nanotubes and Visualization of a Nanotube–Protein Hybrid under Fluorescence Microscope. *Biomacromolecules* **2011**, *12*, 1200–1204.

(31) Prakash, R.; Washburn, S.; Superfine, R.; Cheney, R. E.; Falvo, M. R. Visualization of Individual Carbon Nanotubes with Fluorescence Microscopy Using Conventional Fluorophores. *Appl. Phys. Lett.* **2003**, *83*, 1219–1221.

(32) Cavuslar, O.; Unal, H. Self-Assembly of DNA Wrapped Carbon Nanotubes and Asymmetrical Cyanine Dyes into Fluorescent Nanohybrids. *RSC Adv* **2015**, *5*, 22380–22389.

(33) Clark, M. D.; Subramanian, S.; Krishnamoorti, R. Understanding Surfactant Aided Aqueous Dispersion of Multi-Walled Carbon Nanotubes. *J. Colloid Interface Sci.* **2011**, *354*, 144–151.

(34) Albertorio, F.; Hughes, M. E.; Golovchenko, J. A.; Branton, D. Base Dependent DNA–Carbon Nanotube Interactions: Activation Enthalpies and Assembly–Disassembly Control. *Nanotechnology* **2009**, *20*, 395101.

(35) Ruchira Silva, W.; Keller, E. L.; Frontiera, R. R. Determination of Resonance Raman Cross-Sections for Use in Biological SERS Sensing with Femtosecond Stimulated Raman Spectroscopy. *Anal. Chem.* **2014**, *86*, 7782–7787.

(36) Berezin, M. Y.; Lee, H.; Akers, W.; Achilefu, S. Near Infrared Dyes as Lifetime Solvatochromic Probes for Micropolarity Measurements of Biological Systems. *Biophys. J.* **2007**, *93*, 2892–2899.

(37) Qian, J.; Jiang, L.; Cai, F.; Wang, D.; He, S. Fluorescence-Surface Enhanced Raman Scattering Co-Functionalized Gold Nanorods as near-Infrared Probes for Purely Optical in Vivo Imaging. *Biomaterials* **2011**, *32*, 1601–1610.

(38) Berezin, M. Y.; Zhan, C.; Lee, H.; Joo, C.; Akers, W. J.; Yazdanfar, S.; Achilefu, S. Two-Photon Optical Properties of Near-Infrared Dyes at 1.55 μm Excitation. *J. Phys. Chem. B* **2011**, *115*, 11530–11535.

(39) Dietze, D. R.; Mathies, R. A. Molecular Orientation and Optical Properties of 3,3'-Diethylthiatricarbocyanine Iodide Adsorbed to Gold Surfaces: Consequences for Surface-Enhanced Resonance Raman Spectroscopy. *J. Phys. Chem. C* **2015**, *119*, 9980–9987.

(40) Würthner, F.; Kaiser, T. E.; Saha-Möller, C. R. J-Aggregates: From Serendipitous Discovery to Supramolecular Engineering of Functional Dye Materials. *Angew. Chem., Int. Ed.* **2011**, *50*, 3376–3410.

(41) Baskaran, D.; Mays, J. W.; Bratcher, M. S. Noncovalent and Nonspecific Molecular Interactions of Polymers with Multiwalled Carbon Nanotubes. *Chem. Mater.* **2005**, *17*, 3389–3397.

(42) Zhang, H.; Chen, H.-J.; Du, X.; Wen, D. Photothermal Conversion Characteristics of Gold Nanoparticle Dispersions. *Sol. Energy* **2014**, *100*, 141–147.

(43) Kang, S.; Herzberg, M.; Rodrigues, D. F.; Elimelech, M. Antibacterial Effects of Carbon Nanotubes: Size Does Matter! *Langmuir* **2008**, *24*, 6409–6413.

(44) Burke, A.; Hasirci, N. *Polyurethanes in Biomedical Applications*; Springer: Boston, MA, 2004; pp 83–101.